

<https://doi.org/10.33472/AFJBS.6.6.2024.5506-5521>



African Journal of Biological Sciences

Journal homepage: <http://www.afjbs.com>



Research Paper

Open Access

Multilevel Deep Learning Approach To Classify Lung Cancer as Per Tumor Node Metastasis Coding

Mrs. Vanita D. Jadhav¹, Dr. Lalit V. Patil²

¹Ph.D.Research Scholar, SKN College of Engineering, Vadgaon, Pune, India

²Professor, SKN College of Engineering, Vadgaon, Pune, India

¹vdjadhav@coe.sveri.ac.in, ²lalitvpatil@gmail.com

Article Info

Volume 6, Issue 6, June 2024

Received: 13 April 2024

Accepted: 10 May 2024

Published: 14 June 2024

doi: 10.33472/AFJBS.6.6.2024.5506-5521

ABSTRACT:

Tumour Node Metastasis (TNM) coding is used to classify lung cancer using a multilevel deep learning approach, which aids in predicting the stage of the disease. Using many deep learning networks at different levels, the multilevel deep learning approach handles complicated issues. In order to classify CT lung scans into three groups of classes, this study developed three unique Tumor-Node-Metastasis categorization methods, as advised by the American Joint Committee on Cancer (AJCC). First, an ideal conditional generative adversarial network (c-GAN) has been established for automated lung segmentation, which includes the juxtapleural nodule and the nodules inside the lung. For the next step, three support vector machine (SVM) classifiers and three distinct deep learning algorithms have been created for cataloging of tumor (T), node (N), and metastasis (M) according to AJCC staging terminology. This learning offers the TNM cataloging, which aids in diagnosis of the cancer stage, in contrast to previous studies on lung cancer classification that concentrated on classifying the given nodule as cancerous or non-cancerous. The suggested classifier outperforms the currently used binary cancer classification algorithm and achieves performance that is comparable to that of the recently created TNM classifier. The suggested method also has the benefit of not requiring human skilled participation to identify the ROI area of the image in order to classify given CT picture into TNM classes.

Keywords: deep learning; support vector machine; lung cancer classification; TNM classes.

© 2024 Mrs. Vanita D. Jadhav, This is an open access article under the CC BY license (<https://creativecommons.org/licenses/by/4.0/>), which permits unrestricted use, distribution, and reproduction in any medium, provided you give appropriate credit to the original author(s) and the source, provide a link to the Creative Commons license, and indicate if changes were made

1. Introduction

A successful treatment outcome and the definition of the course of treatment depend heavily on the ability to predict the level of cancer at the time of diagnosis. The cancer staging system, which was developed to give patients and professionals an individual patient's prognosis and to compare patient classes participating in medical trials to receive ordinary care globally, is used to determine the degree of cancer. Most often used cancer staging method amongst clinicians is the TNM system, which ciphers the extent of the main tumour (T), regional lymph nodes (N), and distant metastases (M). The International Union for Cancer Control (UICC) and AJCC are accountable for keeping it alive. Moreover, it offers a "stage grouping" according to T, N, and M [1, 19]. This study has built a multiple level deep learning classifier for the purpose of classifying lung cancer tumor-node-metastasis (TNM) stages. In order to eliminate an undesired noisy portion from the CT scan, the first level lung segmentation technique uses an optimally tuned Conditional Generative Adversarial Network (c-GAN) algorithm. The following step involves obtaining the deep features needed by each of the three support vector machine (SVM) classifiers using three distinct pre-trained ResNet50 networks. As recommended by the AJCC, the benefit of suggested multiple level classifier is the development of a fully automated TNM classification procedure for the identification of cancer stages. The Cancer Imaging Archive (TCIA) record is used to test and train the suggested algorithms.

2. Literature Survey

Radiologists are finding that computer-aided diagnostic (CAD) technologies facilitate better decision-making. Deep learning techniques and technology are driving a rapid increase in CAD accuracy across all medical imaging domains. Lung cancer is currently diagnosed using a variability of imagery modes, including magnetic resonance imaging (MRI), computed tomography (CT), and PET/PET scans. Among these, CT scans offer sufficient data for the diagnosis and staging of non-small-cell lung cancer. Survey study on lung nodule cataloging using computed tomography (CT) pictures and deep learning procedures states that a large number of studies have been carried out on application of deep learning methods for the discovery of malicious tumours in lung CT images [2]. Lung cancer diagnosis involves two stages: staging Cheng et al. [3], additional examination of the tumor's malignancy, and lesion finding. Segmentation of the lung, candidate nodule detection, false-positive lessening, and classification are the four main phases in lesion detection. The identification of a tumor's malignancy involves three steps: feature extraction, feature subset selection, and classification [2].

2.1 Benign and Malignant Classification Using Patch Approach

Utmost of the previous studies on the discovery of lung cancer focused on differentiating between benign and malignant nodules. These research are shown with region of interest (ROI) patch pictures from the datasets of LIDC and IDRI. Kang and Liu [4] suggested the use of a Multi-view Convolutional Neural Network (MV-CNN) for Binary and Ternary Classification. The multi-view strategy performs more accurately than the single view approach for binary or ternary classifications. Da Silva [5] combined a genetic process with a deep learning method to categorize lung nodules as benign or malignant. The recommended methodology, which made use of the LIDC-IDRI database, has the following metrics: sensitivity, specificity, accuracy, and area under the ROC: 94.66%, 95.14%, 94.78%, and 0.949, respectively. Dey et al. [6] suggested a binary classifier for class label translation of 3D photos, based on a four two-pathway CNN. The proposed CNN included a basic 3D CNN, an upgraded 3D

DenseNet with multiple outputs, a new multi-output network, and a 3D DenseNet. The evaluation of the four networks with the public LIDC-IDRI dataset yielded better results than most existing methods.

Zhao et al. [7] built a cross CNN combining AlexNet and LeNet using layer setting from LeNet and parameter configuration from AlexNet. So as to identify the best CNN network, performance of proposed network was investigated by adjusting various network parameters. The performance of the ideal network yielded accuracy value of 0.8220 and area under the curve of 0.8771.

Xie et al. [8] suggested a lung nodule classifier using texture, shape, and deep model-learned information. To construct the classifier, three descriptors were used: a texture descriptor, a Fourier shape descriptor, and a deep convolutional neural network. Additionally, the recommended approach constructed an AdaBoosted back propagation neural network that can distinguish between nodules using the judgements of three classifiers. As a result, the LIDC-IDRI dataset's performance accomplished an accuracy of 96.65%, 94.45%, and 81.24%, respectively, which was significantly higher than the accuracy attained by other techniques.

Shakeel et al. [9] created a technique to enhance lung image quality and lung cancer diagnosis by reducing misclassification. The TCIA dataset's CT images were cleaned up of noise using the weighted mean histogram equalisation technique. The procedure of intensive clustering to enable segmentation of the required region considerably enhanced the quality of the photographs. The DL model was trained to detect lung cancer with a minimum classification error of 0.038 and an accuracy of 98.42% using various spectral data from the affected region.

2.2 Benign and Malignant Classification Using Whole CT Images

Another method of using all of the CT images by segmenting them to reduce image noise has also been studied in the literature.

Lakshmana prabu et al. [10] presented an automated diagnosis classification method for lungs CT images based on Linear Discriminate Analysis (LDA) and Optimal Deep Neural Network (ODNN). The deep features that were extracted from CT lung images were minimised by using LDR in order to classify binary lung nodules. The combined ODNN and Modified Gravitational Search Algorithm yields sensitivity, specificity, and accuracy rates for lung cancer that are 96.2%, 94.2%, and 94.56%, respectively.

Halder et al. developed a technique for segmenting the lung nodule region using an adaptive morphological filter [11]. The candidate nodule regions were identified using an adaptive morphological filter that utilised the adaptive structural elements. It also improved the accuracy of nodule detection by reducing false positives from the CT slices. The morphological, texture, and intensity-based features were extracted from the nodule found candidate region and used to train the support vector machine classifier for lung nodule detection applications. The proposed method yielded results with sensitivity, specificity, and accuracy of 94.88%, 93.45%, and 94.27%, respectively, using the LIDC/IDRI dataset.

Nanglia et al. [12] developed a hybrid method that combines a support vector machine and a feed-forward back propagation neural network for the classification of lung cancer. The dataset preparation block, the feature extraction block using the SURF approach and additional optimisation using the genetic algorithm, and the terminal block that performs the classification using FFBPNN were the three blocks that made up the classification strategy. The recommended method's overall classification accuracy was 98.08%.

Tiwari et al. [13] projected a lung cancer detection method based on a Mask Unit (MU) based 3FCM algorithm and a Target based Weighted Elman DL Neural Network (TWEDLNN). Additionally, the proposed algorithm made use of the Modified Clip limit-

based Contrasts Limited Adaptive Histograms Equalisation (MC-CLAHE) for contrast enhancement and Feature Extraction (FE), the Geometric mean-based Otsu Thresholding (GOT) for image segmentation, and the MU-based FCM procedure for lung nodule detection. In order to confirm that TWEDLNN is a more effective lung cancer detection approach, the effectiveness of the recommended algorithm was assessed using the LIDC-IDRI database and compared with existing methods. As a consequence, the suggested task's accuracy increased by 96%.

Mohana Priya and Venkatesan provided fusion of lung CT and PET images for segmentation and classification [14]. The proposed method consisted of four basic steps: post-pre-processing, fused picture classification, lung image fusion, and lung segmentation. Initially, a dual-tree m-band wavelet (DTWT) was used to deconstruct the raw CT/PET images. These fragmented images were then combined using the deep learning method. The lower frequency sub-band coefficients were adjusted to zero and the higher frequency components were used for reconstruction. After that, the segmentation was done using the clustering-based thresholding method. Following the removal of the unwanted microscopic sections using morphological operations, the lung region was identified. Finally, a SVM classifier with a greater cataloging accuracy of 99% was used to classify the intensity and texture-based characteristics.

2.3 TNM Classification

Compared to early work on the classification of selected lung nodules as benign and malignant, the paradigm change is developing lung classification algorithms for classifying it in TNM classes using CT scans.

By Kirienko et al. [15], the CNN-based lung cancer classifier was unveiled. It consists of two neural networks required for FDG-PET/CT image feature extraction and classification. The CNN classifier uses the higher-level properties for binary classification between the T1-T2 class and the T3-T4 class. The test yielded values for accuracy, recall, specificity, and AUC of 90%, 47%, 67%, and 0.68, respectively.

The CNN-based approach for nodule identification proposed by Paul et al. [16] was recommended for the follow-up of cancer patients. This technique was developed using three CNN models, which improved its accuracy and flexibility. Finally, augmented images were used to train and assess these networks for the purpose of classifying T0, T1, and T2 classes. As such, their predictive power for the occurrence of lung cancer at T2 from a different test group was 90.28% accurate with an accuracy of 0.960.

Zhao et al. [17] established a 3D neural network to predict lymph node metastasis of T1 lung adenocarcinoma using inputs from CT images and prior clinical knowledge. For the suggested network's training and validation, 401 cases were selected, whilst 100 examples were picked for testing. Finally, the effectiveness of the proposed method was compared with the logistic regression integration model, which was developed as a single deep learning model without using previous clinical knowledge, and the radiomics method and radiologists' manual evaluation of it. The recommended network beat the single deep learning model (0.880), the logistic regression integration model (0.904), and the radiomics method (0.891) with an AUC performance score of 0.926.

Mandal and Moitra [18] introduced a one dimensional CNN model for the automatic staging and grading of NSCLC. The segmented tumour images were loaded into a hybrid feature extraction and detection system. These variables, along with clinical TNM stage and histological grade data, were used to train a 1-D CNN model using data from The Cancer Imaging Archive (TCIA) database. The algorithm's 94-59% success rate is a major improvement over earlier algorithms. This investigation's main constraint was the

requirement for physical skilled intervention in order to divide tumour, will prevent the procedure from being automated. The correctness of these algorithms is dependent on the quality of nodule segmentation. It will be challenging to predict cancer early if little nodules are overlooked.

3. Methodology

3.1 Multi-Level Deep Learning Approach for TNM classification

The creation of a multi-level deep learning approach is gaining traction since it increases process efficiency overall by enhancing performance at each level. Regions of interest (ROI) photographs acquired with the assistance of specialists are used by existing lung cancer algorithms for algorithm testing and training. The two-fold classification of provided nodule patches as malignant or benign has been the main focus of these existing systems. Oncologists and radiologists who treat lung cancer, however, base their classification strategy on the Tumor-Node-Metastasis (TNM) classification. The suggested multi-level deep learning technique is depicted in Figure 1. It develops a fully autonomous TNM classifier by utilizing different levels of deep learning algorithms. First, to aid in process automation, a c-GAN is created for segmentation of lung. The segmentation procedure makes sure that all of the lung image's nodules are included and that non-lung areas are removed. In order to extract the deep features needed in relation to tumor-node-metastasis, segmented lung picture is fed to 3 separate Resnet50 algorithm that have already undergone pre-training. To categorize these structures into TNM, each Resnet50 is followed by an independent support vector machine (SVM).

This multilayer classifier simultaneously classifies each CT image that is fed as input into three distinct sets of classes. According to AJCC code, the classification acquired in these three classes aids in determining the cancer stage. The TNM classes taken into account in the study and how the classes relate to different stages of cancer are displayed in Table 1. For instance, the stage of cancer is IIIA if the CT scan is categorized as T2 for tumour, N2 for node, and M0 for metastasis. In a similar vein, the stage of cancer is IVA if provided image is categorized as T1 for tumour, N0 for node, and M1a for metastasis. These phases are helpful in determining the patient's best course of treatment and in assessing the likelihood of survival. Additionally, this method is helpful in assessing a patient's reaction to specific medicines.

Formulation of the segmentation level deep learning algorithm, deep feature Extraction level deep learning algorithms and SVM classifiers is explained in the following subsections.

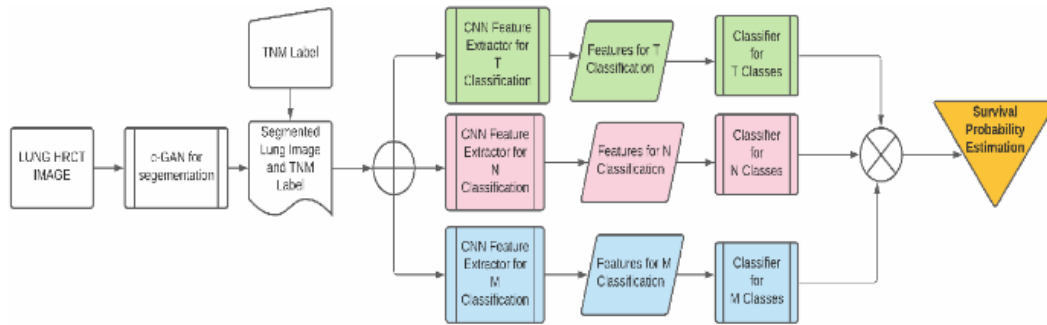


FIGURE 1: Multi-Level Deep Learning for Survival Probability Estimation in TNM Lung Classification.

Table 1: The relationship between TNM Classes and stages of cancer [19]

	N0	N1	N2	N3
T1	IA	IIB	IIIA	IIIB
T2	IIA	IIB	IIIA	IIIB
T3	IIB	IIIA	IIIB	IIIC
T4	IIIA	IIIA	IIIB	IIIC
M1a	IVA	IVA	IVA	IVA
M1b	IVA	IVA	IVA	IVA
M1c	IVB	IVB	IVB	IVB

3.2 Optimal c-GAN for Lung Segmentation

Taguchi optimization approach is employed to enhance the presentation of the c-GAN architecture [20]. The Taguchi optimization strategy is used to select and tune the c-GAN network in order to maximize the segmentation performance parameters of the Jaccard index (J) and dice similarity coefficient (DSC).

The architecture's performance can be adjusted by choosing the right amount of MSFE inception blocks. Additionally, the network is fine-tuned using Adam's optimization parameters. The network has been fine-tuned for the suggested approach for segmenting images with nodules by utilizing an L27 orthogonal array.

3.3 Deep Learning-based Classifier

Three distinct pre-trained Resnet50 algorithms are used to abstract the deep features from the segmented lung pictures with respect to the TNM classes. In medical picture feature extraction procedure, when image databases are scarce, the pre-trained Resnet50 is gaining popularity. This technique can be efficiently trained to acquire deep features with a smaller picture collection because it has only used a section of the ImageNet database (<http://www.image-net.org>) [21].

Based on the deep features extracted from a specific layer of the Resnet50, the powerful stochastic classifier known as the support vector machine is utilised to classify different classes of TNM categories. In each layer, the network collects different deep features related to classification before moving on to the next layer. GPU memory can accommodate the picture dataset, and the activation has a minibatch size of 64.

3.4 Effectiveness of c-GAN in the Lung Segmentation Process

The Cancer Imaging Archive (TCIA) database is used to train and evaluate the suggested algorithms [23, 24]. The database includes CT scans of people with lung cancer that have

annotations pointing to the location of the tumour. These CT scans have a resolution of 512 x 512. The five academic thoracic radiologists who specialise in lung cancer have annotated the database. The TNM classification has been applied to the patient data. About 10–20 CT pictures of each patient are chosen for this investigation based on the annotations that are currently accessible. The following is a summary of the practical significance of TNM classes:

3.4.1 Tumor (T) classification:

- T1-Tumor Size ≤ 3 cm,
- T2-Tumor Size >3 cm to ≤ 5 cm,
- T3- Tumor Size >5 cm to 7cm ,
- T4-Tumor Size >7 cm.

3.4.2 Nodes (N) classification:

- N0- regional lymph node involvement,
- N1-nodes are ipsilateral nodes within the lung up to hilar nodes,
- N2-nodes represent ipsilateral mediastinal or subcarinal lymphadenopathy,
- N3-nodes represent contralateral mediastinal or contralateral hilar lymphadenopathy or scalene or supraclavicular nodes.

3.4.3 Metastases (M) classification:

- M0-No distant metastases and
- M1- Distant metastases:
 - 1.M1a-Regional metastatic disease defined as malignant pleural
 - 2.M1b-solitary extrathoracic metastasis
 - 3.M1c- Multiple extrathoracic metastases

By increasing performance parameters DSC and J, the network's ideal parameters are found. Approximately 600 randomly selected CT pictures are used for training the segmentation algorithm in the 27 studies, and 1000 CT pictures from each of the aforementioned classes are used for testing. The model's other parameters are comparable to the [25]. To train the suggested network for precise lung field segmentation, a PC equipped with an NVIDIA GTX 1080 8 GB GPU and an Intel Core i7 processor running at 4.20 GHz is utilised. The MSFE architecture yields the best network performance when the images are downsampled to a 16 by 16 resolution.

Performance of the loss function during the training stages for the segmentation of the lung portion that includes the tumour is displayed in Figure 2. These graphs demonstrate that only the early steps of the generator and discriminator loss functions exhibit convergence. But at about 20,000 steps, the L1 loss function converges.

The c-GAN network, which has been optimally constructed in terms of performance, is compared to the most advanced deep networks currently in use, namely NMF [26], UNet [27], and ResNet [21]. All the techniques often produce performance that is passably excellent and free of nodules. But the segmentation performance begins to suffer when there are nodules. The average DSC and J performances of the best c-GAN, which were obtained using 100 randomly selected images from each of the four classes—T1, T2, T3, and T4—are contrasted in Table 2 (different from training images). The segmentation performance of the suggested segmentation approach and the current state-of-the-art algorithms of CT images with different lung tumours are displayed in this table. Appendix A displays the comprehensive performance analysis for all 100 photos across four classes. The suggested segmentation scheme performs better than the current approaches, according to the results. The suggested algorithm also has the benefit of producing better outcomes irrespective of the location and size of nodules. However, size and location of the nodule affects the other approaches.

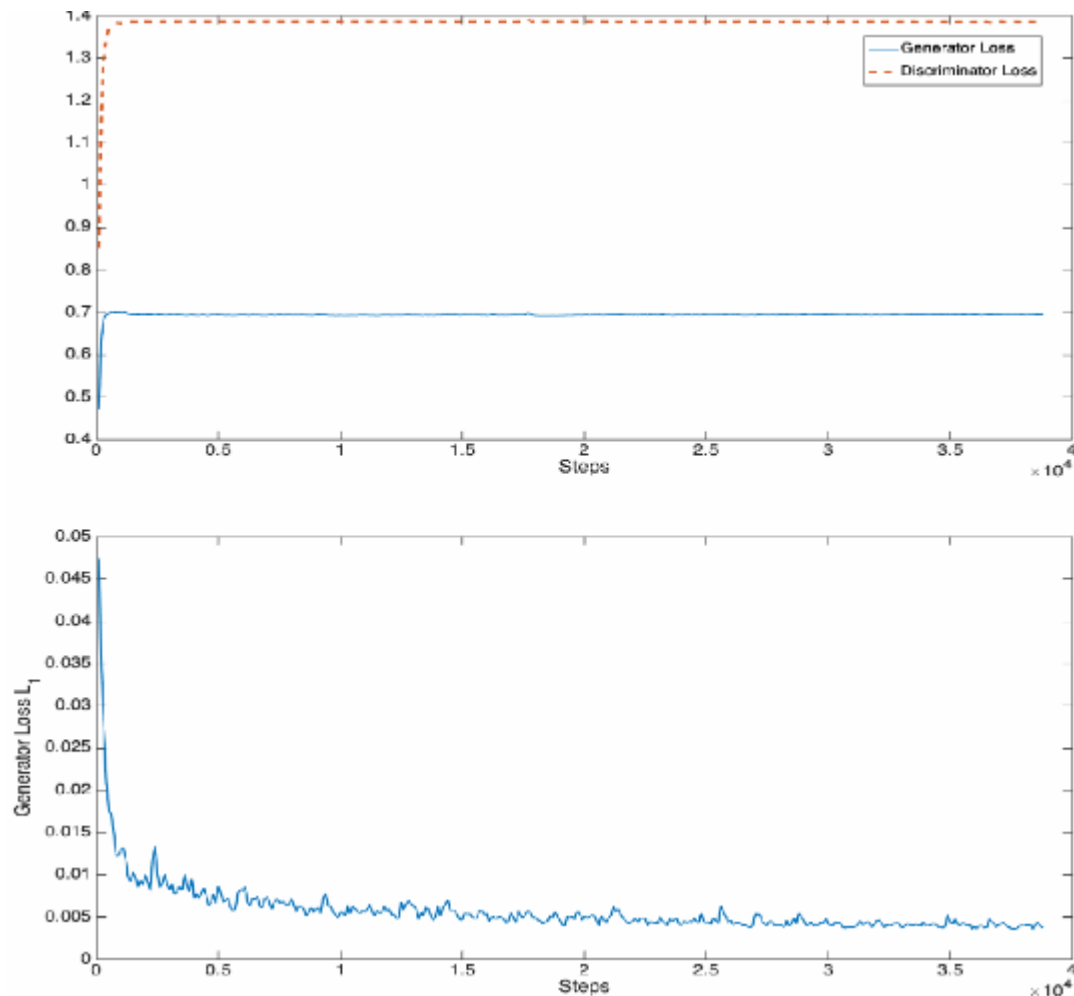


FIGURE 2: Loss function plots for training of optimal c-GAN

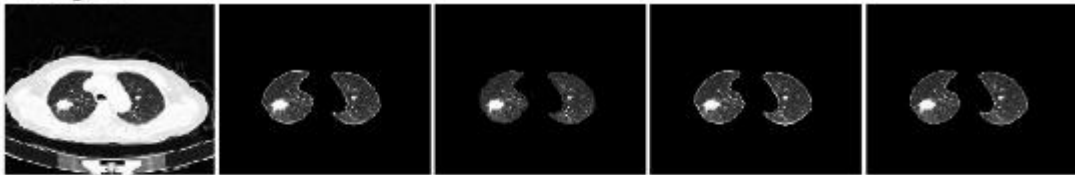
Segmentation routine study of an optimally modified c-GAN for a variety of dangerous pictures belonging to the T1, T2, T3, and T4 modules is displayed in Fig's 3–6. These illustrations demonstrate that the suggested C-GAN algorithm is capable of effectively segmenting pictures with varying nodule sizes as well as the lung when a juxtapleural nodule is present. The segmentation performance algorithm also identified instances where it is challenging to distinguish between the scanning machine's light and lung nodule. Unet is unable to precisely capture nodule morphologies, while NMF performs badly in all four sets of pictures by ignoring the interior and juxtapleural nodules. Resnet accurately segments the lung portion by adding every node, giving the suggested segmentation method a reasonably matching performance. However, in certain instances, Resnet is unable to accurately capture the nodules. For instance, sample 3 for the T3 class somewhat overrates the juxtapleural node, while samples 2 and 3 for the T4 class show that Resnet is unable to accurately capture the inner nodule and the juxtapleural nodule. The effectiveness of the segmentation method contributes to process automation and enhances classification performance by lowering background noise in CT images.

Table 2: Comparative performance assessment of average DSC and J for c-GAN and current methods for segmentation of lung.

Tumor	Performance	Proposed system	NMF	UNet	Resnet
T1	DSC	0.9922	0.8574	0.9631	0.9693
	J	0.9847	0.8005	0.9364	0.9489

T2	DSC	0.9851	0.9290	0.9795	0.9847
	J	0.9708	0.8724	0.9794	0.9700
T3	DSC	0.9827	0.9112	0.9617	0.9767
	J	0.9662	0.8395	0.9600	0.9555
T4	DSC	0.9757	0.8793	0.9504	0.9762
	J	0.9529	0.8034	0.9075	0.9540
Average	DSC	0.9839	0.8942	0.9637	0.9767
	J	0.9686	0.8290	0.9458	0.9571

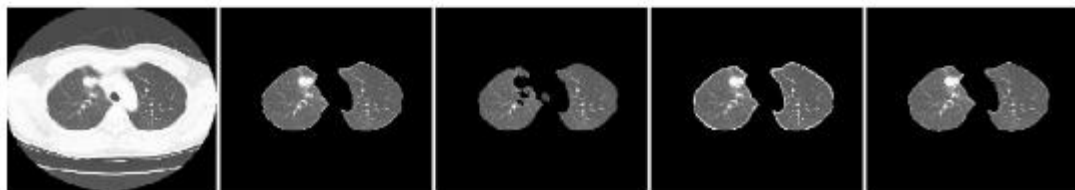
Sample 1



Sample 2



Sample 3



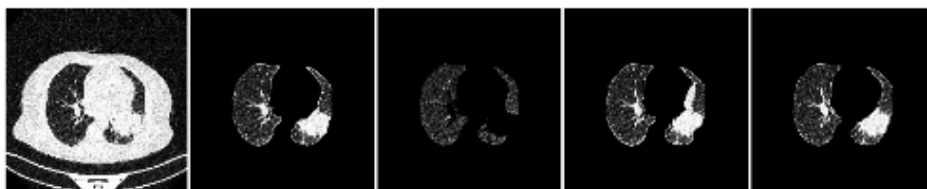
CT Image Projected NMF Unet Resnet Technique

FIGURE 3: Qualitative segmentation performance assessment of T1 class CT imageries

FIGURE 3.3: 3.5 Performance of Deep Learning-based TNM Classifier

Three different Resnet50 networks with each followed by different SVM algorithms have been developed for classifying T1, T2, T3 and T4 classes of Tumor (T), N0, N1, N2 and N3 classes of Node (N) and M0, M1a, M1b and M1c classes of Metastasis (M). Though each segmented image will have three TNM class labels

Sample 1



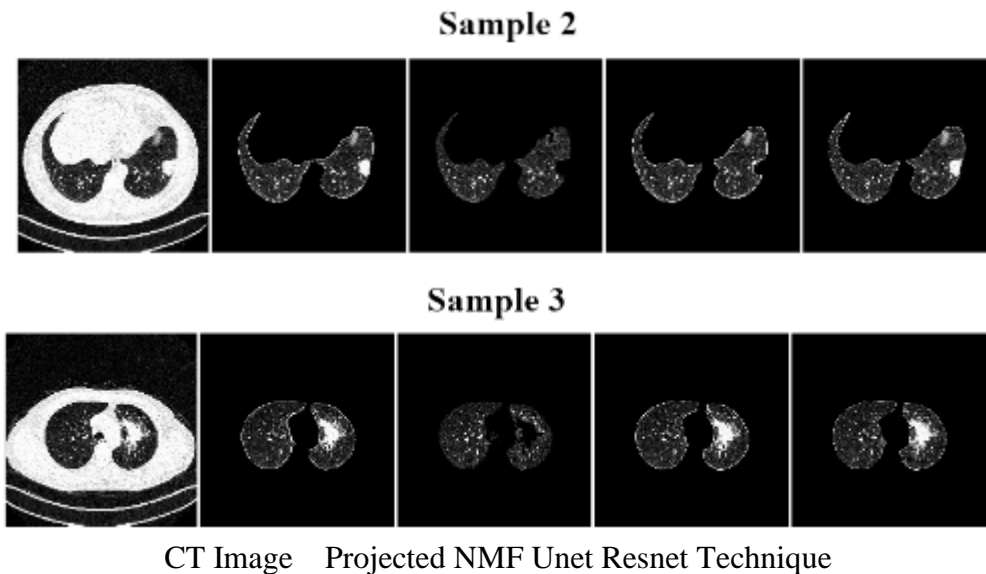
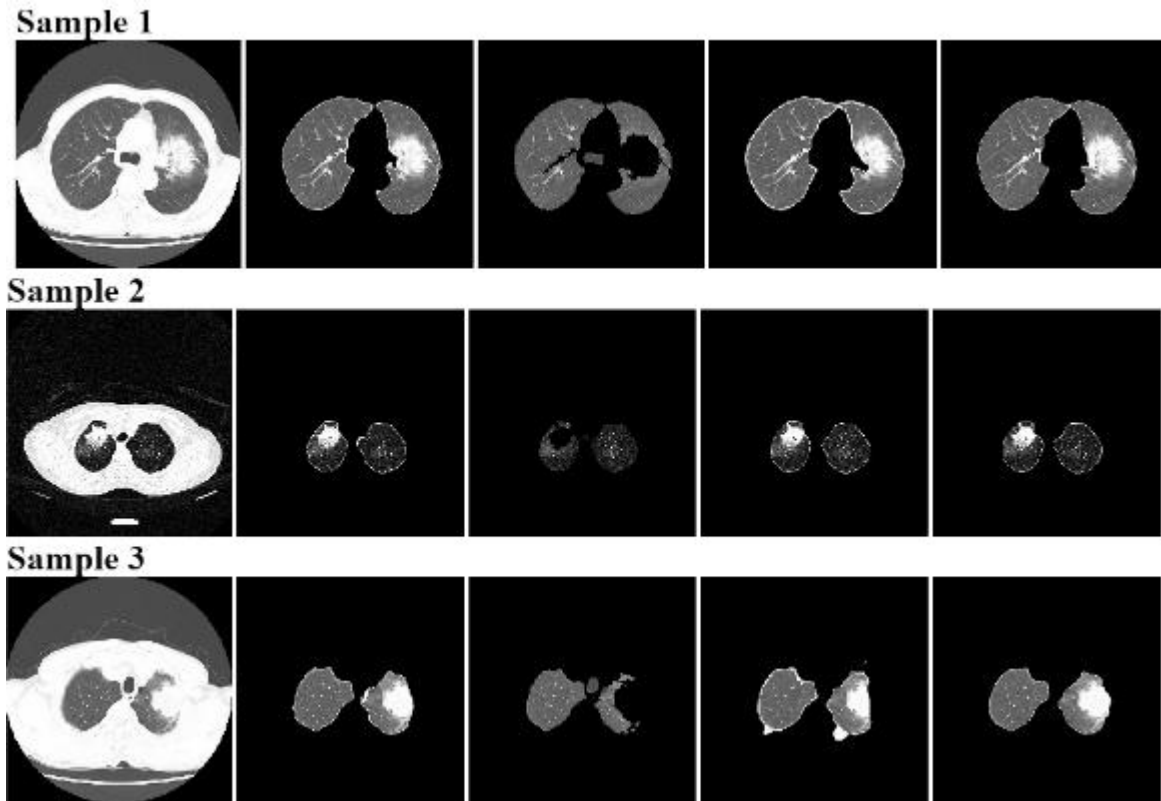


FIGURE 4: Qualitative segmentation performance assessment of T2 class CT imageries

Three different databases for each classification approach have been prepared to avoid confusion during training and testing. The CT images of 512 x 512 were resized to 224 x 224 dimension during the argumentation process. These images are passed to pre-train Resnet50 for extracting the deep features. At this stage, appropriate feature layer selection becomes important for improving classification performance. The weights of earlier layers are frozen in the pre-trained network, which are not updated during the fine-tuning stage. The transfer learning techniques used for Resnet50 becomes advantageous for such problems as it removes the drawback of the shortage of radiological images required to improve deep learning performance. This transfer learning process effectively develops Classification algorithms less training data of medical images. Before the classifier's detailed performance analysis, the influence of feature layer selection on the classifier accuracy is studied. Out of the trials conducted using the selection of features layers as fcc1000, res5c branch2b, res5c branch2c, avg pool and bn5c branch2a, SVM classifier gives the best result for the deep features selected atbn5c branch2a.

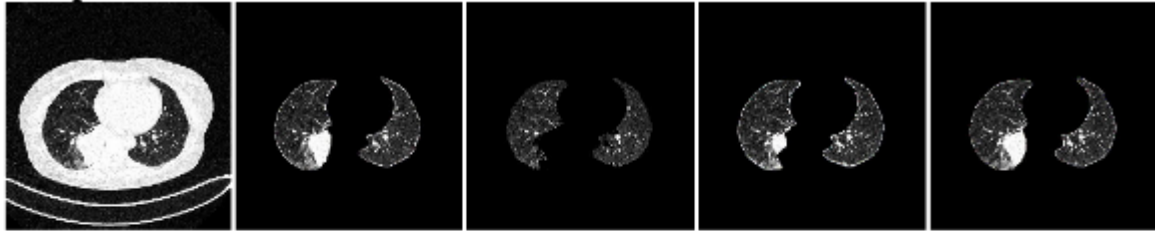


CT Image Projected Technique NMF Unet Resnet
 FIGURE 5: Qualitative segmentation performance assessment of T3 class CT images.

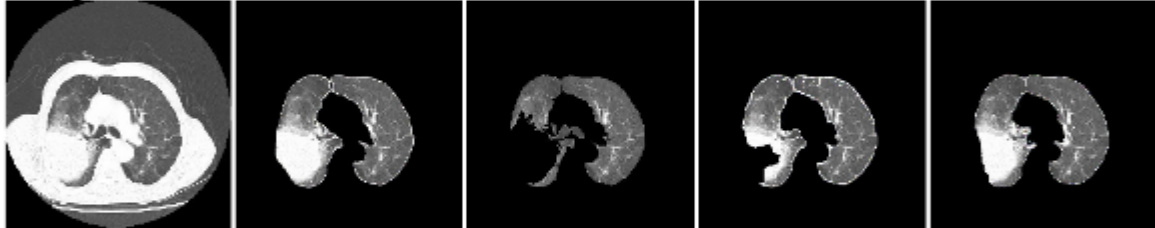
Tumour (T) categorization performance is displayed in Table 3. The system performed well even for classifying the lowest size of the tumour, as seen by the T1 class's maximum performance of 97.32%. The increased classification accuracy for a smaller tumour suggests that this approach can be helpful in the early detection of cancer. About 2-3% of the remaining classes are somewhat confused with the nearby classes. The Tumour classification approach has an average classification performance of approximately 94.70%. Table 4 displays the effectiveness of the Node (N) classification strategy. The N3 class has the best classification performance, at 100%. The N1 class has the lowest accuracy because it confuses with the adjoining N2 class by 5.67%. N2 and N4, the remaining two classes, provide somewhat accurate results. The Node classification approach has an average performance of 95.78%.

Similarly, the effectiveness of the Metastasis (M) classification approach is displayed in Table 5. The fact that the M0 class result demonstrates 100% accuracy suggests that the early stages of cancer types I, II, and III can be predicted with accuracy. The M1a class provides 100% accuracy, but the M1b class significantly misidentifies the M1a class by 2.31%. Since M1a and M1b belong to the same IVA cancer stage, this confusion won't have an impact on the performance of the cancer stage estimation. The Metastasis (M) classification technique has an average performance of approximately 99.23%.

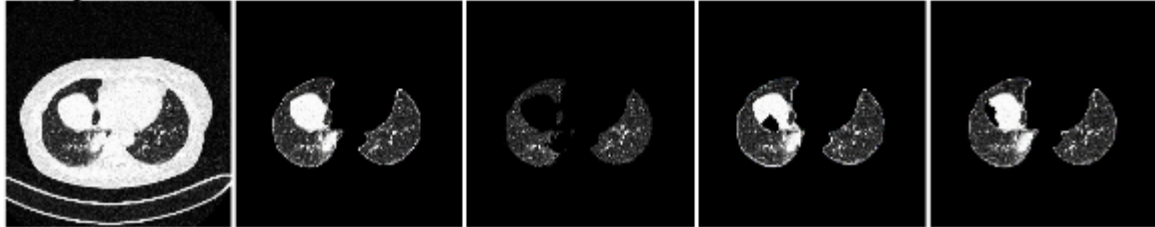
Sample 1



Sample 2



Sample 3



CT Image Projected Technique NMF Unet Resnet

FIGURE 6: Qualitative segmentation performance assessment of T4 class CT images.

The suggested multi-level deep learning-based method's classification performance is compared with previous literature work in Table 6. The majority of literature approaches concentrate on binary classification as benign and malignant, together with ROI patches. For binary classification, the suggested method performs considerably better than all ROI photos combined. Moreover, the suggested technique outperforms the newly created 1-D CNN based TNM classification strategy in terms of performance. The suggested method has an advantage over all previous approaches in that it uses a given CT image to automate TNM categorization, saving diagnostic time so that early therapy can be started and successful treatment outcomes can be achieved.

Table 3: Confusion matrix for cataloging of Tumour (T).

Actual Cases	Prediction (%)			
	T1	T2	T2	T4
T1	97.321	1.881	0.271	0.540
T2	2.270	91.941	3.020	2.771
T3	1.830	2.250	93.530	2.390
T4	0.441	0.440	3.101	96.021

Table 4: Confusion matrix for cataloging of Nodule (N).

Actual Cases	Prediction (%)			
	N0	N1	N2	N3
N0	91.990	5.671	0.000	2.341
N1	1.551	96.770	0.131	1.550
N2	0.000	0.000	100.000	0.000

N3	2.801	2.041	0.000	95.171
----	-------	-------	-------	--------

Table 5: Confusion matrix for cataloging of Metastasis (M).

Actual Cases	Prediction (%)			
	M0	M1a	M1b	M1c
M0	100.000	0.000	0.000	0.000
M1a	0.000	100.000	0.000	0.000
M1b	0.000	2.310	97.690	0.000
M1c	0.000	0.000	0.750	99.250

Table 6: Comparison of projected algorithm with previous CNN founded Classifiers

Method	Technique	Average
Zhao et al. [84]	Binary cataloging, ROI area extraction	81.79%
Dey et al. [14]	Binary cataloging, ROI area extraction	89.90%
Liu and Kang [43]	Binary cataloging, ROI area extraction	91.59%
Xie et al. [80]	Binary cataloging, ROI area extraction	92.69 %
Ma et al. [45]	Binary cataloging, ROI area extraction	81.78%
Paing and Choomchuay [53]	Binary cataloging, ROI area extraction	89.67%
Moitra and Mandal [48]	TNM Cataloging, de-noised by the Gaussian Blurring method	95.99 %
Proposed approach	TNM Classification, using Multilevel deep learning based involuntary lung segmentation and classification	96.64 %

4. Conclusion

The stage (extent) of the cancer must be determined so as to treat non-small cell lung cancer (NSCLC). AJCC recommends by means of the Tumor-Node-Metastasis (TNM) cataloging to determine the disease stage. As recommended by the AJCC, this study has created three distinct categorization methods for Tumor-Node-Metastasis in order to categorise CT lung scans into three groups of classes. An optimised c-GAN network has been constructed for automatic lung segmentation, encompassing the nodules within the lung and juxtapleural nodule, at the first level. This methodology is similar to the ILD classification method. For the next step, three SVM classifiers and three distinct deep learning algorithms have been created for the cataloging of tumour (T), nodal (N), and metastasis (M) according to the AJCC staging terminology. The following conclusions are drawn from the multilevel Lung Cancer classification approach study:

1. To detect the tumour size (T), nodule location (N), and metastases level (M), a multilayer deep learning founded method is created to segment provided CT picture and categorise the picture into 3 diverse ways of classes. This study has concentrated on TNM classification, which aids in the diagnosis of the cancer stage, as opposed to previous studies on lung cancer classification, which identified the given nodule as cancerous or non-cancerous. Using the best-tuned c-GAN, the initial level segmented the lungs from provided CT image, removing background noise from the chest region and included nodes of various sizes.
2. To acquire deep features associated with the TNM classes at the ensuing levels, three Resnet50 networks have been employed. An SVM classifier follows each of the Resnet50 networks to classify the CT picture into classes based on metastasis level (M), tumour size (T), and node location (N). The suggested classifier outperforms the currently used binary

cancer classification algorithm and achieves performance that is comparable to that of the recently created TNM classifier.

3. The suggested method also has the benefit of classifying the provided CT image into TNM classes without the need for human expert selection or clipping of the ROI area of the picture. This study also demonstrates how level-wise error minimization using deep learning procedures at the multilayer has enhanced system performance.

5. References

1. Edge, S.B., C. C. (2010). The american joint committee on cancer: the 7th edition of the AJCC cancer staging manual and the future of TNM. *Ann Surg Oncol*, 17:1471–1474.
2. Naik, A., E. D. (2021). Lung nodule classification on computed tomography images using deep learning. *Wireless Pers Commun*, 116:655–690.
3. Cheng, J. Z., Ni, D., Chou, Y. H., and (2016). Computer-aided diagnosis with deep learning architecture: Applications to breast lesions in us images and pulmonary nodules in ct scans. *Sci Rep*, 6:24454.
4. Liu, K. and Kang, G. (2017). Multiview convolutional neural networks for lung nodule classification. *International Journal of Imaging Systems and Technology*, 27(1):12–22.
5. da Silva, G. and da Silva, N. (2017). Lung nodules diagnosis based on evolutionary convolutional neural network. *Multimed Tools Appl*, 76:19039–19055.
6. Dr.Sapna Sukrut Deo et al. (2019). JUDICIAL REFORM: COMBATTING DELAYED JUSTICE. *International Journal of Advanced Science and Technology*, 28(15), 340 - 343.
7. Dey, R., Lu, Z., and Hong, Y. (2018). Diagnostic classification of lung nodules using 3d neural networks. In 2018 IEEE 15th International Symposium on Biomedical Imaging (ISBI 2018), pages 774–778.
8. Dr. Sapna Sukrut Deo, Prof. Dr. Pooja Prashant Narwadkar, Dr. Madhura Kalamkar, Dr. Aishwarya Yadav and Mr. Jatin Sethi (2024), Affecting computing for social justice. *African Journal of Biological Sciences (South Africa)*. 6(6), 1610-1614.
9. Zhao, X., Liu, L., Qi, S., and (2018). Agile convolutional neural network for pulmonary nodule classification using CT images. *Int J CARS*, 13:585–595.
10. Xie, Y., Zhang, J., Xia, Y., Fulham, M., and Zhang, Y. (2018). Fusing texture, shape and deep model-learned information at decision level for automated classification of lung nodules on chest CT. *Information Fusion*, 42:102–110.
11. Dr.Sapna Sukrut Deo et al. (2019). RIGHT TO PRIVACY BETWEEN HUSBAND AND WIFE. *International Journal of Advanced Science and Technology*, 28(15), 337 - 339.
12. Shakeel, P. M., Burhanuddin, M., and Desa, M. I. (2019). Lung cancer detection from CT image using improved profuse clustering and deep learning instantaneously trained neural networks. *Measurement*, 145:702–712.
13. Lakshmanprabu, S., Mohanty, S. N., K., S., N., A., and Ramirez, G. (2019). Optimal deep learning model for classification of lung cancer on CT images. *Future Generation Computer Systems*, 92:374–382.
14. Halder, A., Chatterjee, S., Dey, D., Kole, S., and Munshi, S. (2020). An adaptive morphology based segmentation technique for lung nodule detection in thoracic CT image. *Computer Methods and Programs in Biomedicine*, 197:105720.
15. Nanglia, P., Kumar, S., Mahajan, A. N., Singh, P., and Rathee, D. (2020). A hybrid algorithm for lung cancer classification using SVM and neural networks. *ICT Express*.

16. Tiwari, L., Raja, R., Awasthi, V., Miri, R., Sinha, G., Aliana, M. H., and Polat, K. (2021). Detection of lung nodule and cancer using novel mask-3 FCM and TWEDLNN algorithms. *Measurement*, 172:108882.
17. Sarda, M., Deshpande, B., Deo, S., & Karanjkar, R. (2018). A comparative study on Maslow's theory and Indian Ashrama system." *International Journal of Innovative Technology and Exploring Engineering*, 8(2), 48-50.
18. MohanaPriya, R. and Venkatesan, P. (2021). An efficient image segmentation and classification of lung lesions in pet and CT image fusion using DTWT incorporated SVM. *Microprocessors and Microsystems*, 82:103958.
19. Kirienko, M., Sollini, M., Silvestri, G., Mognetti, S., Voulaz, E., Antunovic, L., Rossi, A., Antiga, L., and Chiti, A. (2018). Convolutional neural networks promising in lung cancer t-parameter assessment on baseline FDG-PET/CT. *Contrast Media and Molecular Imaging*, 2018:1382309.
20. Deo, S., & Deo, S. (2019). Cybersquatting: Threat to domain name. *International Journal of Innovative Technology and Exploring Engineering*, 8(6), 1432-1434.
21. Paul, R., Schabath, M., Gillies, R., Hall, L., and Goldgof, D. (2020). Convolutional neural network ensembles for accurate lung nodule malignancy prediction 2 years in the future. *Computers in Biology and Medicine*, 122:103882.
22. Zhao, X., Wang, X., Xia, W., Li, Q., Zhou, L., Li, Q., Zhang, R., Cai, J., Jian, J., Fan, L., Wang, W., Bai, H., Li, Z., Xiao, Y., Tang, Y., Gao, X., and Liu, S. (2020). A cross-modal 3D deep learning for accurate lymph node metastasis prediction in clinical stage T1 lung adenocarcinoma. *Lung Cancer*, 145:10-17.
23. Deo, S., & Deo, D. S. (2019). Domain name and its protection in India. *International Journal of Recent Technology and Engineering*.
24. Moitra, D. and Mandal, R. (2020). Classification of non-small cell lung cancer using one-dimensional convolutional neural network. *Expert Systems with Applications*, 159:113564.
25. Detterbeck, F. C. (2018). The eighth edition TNM stage classification for lung cancer: What does it mean on main street? *The Journal of Thoracic and Cardiovascular Surgery*, 155(1):356-359.
26. Sinha, S., Deshpande, B., Deo, S., & Vedpathak, S. (2019). Potential appeal mechanism by consent: Arbitration. *International Journal of Recent Technology and Engineering*.
27. Roy, R. (2001). *Design of experiments using the Taguchi approach: 16 steps to product and process improvement*. Wiley, New York.
28. He, K., Zhang, X., Ren, S., and Sun, J. (2016). Deep residual learning for image recognition. *Proceedings of the IEEE Conference on Computer Vision and Pattern Recognition*, pages 770-778.
29. Sethy, P. K., Barpanda, N. K., Rath, A. K., and Behera, S. K. (2020). Deep feature based rice leaf disease identification using support vector machine. *Computers and Electronics in Agriculture*, 175:105527.
30. Li, P., Wang, S., Li, T., Lu, J., HuangFu, Y., and Wang, D. (2017). A large-scale CT and PET/CT dataset for lung cancer diagnosis. *The Cancer Imaging Archive*, 76:19039-19055.
31. Clark, K., Vendt, B., Smith, K., Freymann, J., Kirby, J., Koppel, P., Moore, S., Phillips, S., Maffitt, D., Pringle, M., Tarbox, L., and Prior, F. (2013). The cancer imaging archive (TCIA): Maintaining and operating a public information repository. *Journal of Digital Imaging*, 26(6):045-1057.
32. Isola, P., Zhu, J.-Y., Zhou, T., and Efros, A. A. (2017). Image-to-image translation with conditional adversarial networks. In *2017 IEEE Conference on*

- Computer Vision and Pattern Recognition (CVPR), pages 5967–5976. IEEE.
33. Hosseini-Asl, E., Zurada, J. M., Gimelfarb, G., and El-Baz, A. (2016). 3-D lung segmentation by incremental constrained nonnegative matrix factorization. *IEEE Transactions on Biomedical Engineering*, 63(5):952–963.
 34. Ronneberger, O., Fischer, P., and Brox, T. (2015). U-Net: Convolutional networks for biomedical image segmentation. In Navab, N., Hornegger, J., Wells, W. M., and Frangi, A. F., editors, *Medical Image Computing and Computer-Assisted Intervention – MICCAI 2015*, pages 234–241, Cham. Springer International Publishing.
 35. T. M. Kulkarni and A. O. Mulani (2024). Deep Learning Based FaceMask Detection: An Approach to Reduce Pandemic Spreads. *African Journal of Biological Sciences (South Africa)*. 6(6), 783-795.
 36. Birajadar Ganesh Basawaraj, Altaf Osman Mulani, Osamah Ibrahim Khalaf, Nasren Farhah, Pravin G. Gawande, Kinage Kishor; Abdullah Hamad Abdulsattar (2024). Epilepsy Identification using Hybrid CoPrO-DCNN Classifier. *International Journal of Computing and Digital Systems*. 16(1).
 37. Kolhe, V. A., Pawar, S. Y., Gohari, S., Mulani, A. O., Sundari, M. S., Kiradoo, G., ... & Sunil, J. (2024). Computational and experimental analyses of pressure drop in curved tube structural sections of Coriolis mass flow metre for laminar flow region. *Ships and Offshore Structures*, 1-10.
 38. Mulani, A. O., Birajadar, G., Ivković, N., Salah, B., & Darlis, A. R. (2023). Deep learning based detection of dermatological diseases using convolutional neural networks and decision trees. *Traitement du Signal*, 40(6), 2819-2825.
 39. Mane, P. B., & Mulani, A. O. (2019). High throughput and area efficient FPGA implementation of AES algorithm. *International Journal of Engineering and Advanced Technology*, 8(4).